Performance Analysis and Optimization of a Designed 635*nm* $Ga_{0.5}In_{0.5}P/(Al_{0.7}Ga_{0.3})_{0.5}In_{0.5}P$ MQW SCH Red Laser by Varying Differential Gain

Tawsif Ibne Alam[a] , **Rinku Basak**[b]

[a] Department of EEE, Faculty of Engineering, American International University-Bangladesh (AIUB), Banani, Dhaka-1213, Bangladesh.
tawsif.ibne.alam@gmail.com, treblz.89@gmail.com
[b] Assistant Professor and Head (Graduate Program), Department of EEE, Faculty of Engineering, American International University-Bangladesh (AIUB), Banani, Dhaka-1213, Bangladesh.
rinku_biju@yahoo.com, rinku@aiub.edu

Abstract. In this work, the effects of variation of the differential gain on the performance characteristics of a GaInP - based 635*nm* multiple quantum well (MQW) separate confinement heterostructure (SCH) Red laser have been obtained through computations. The peak material gain of $Ga_{0.5}In_{0.5}P/(Al_{0.5}Ga_{0.5})_{0.5}In_{0.5}P$ MQW edge emitting laser has been obtained theoretically and has been used for analyzing the performance of the designed double-heterostructure laser under the effects of variation of differential gain. A maximum output power of 71.18 *mW* and a maximum modulation bandwidth of 13.85 GHz have been obtained for this designed laser at 64 *mA* injection current at 300K, where, the differential gain is $5.1 \times 10^{-16}\ cm^2$. Furthermore a performance analysis with variation in the differential gain reveals that the maximum allowable differential gain at 300K is $6.7 \times 10^{-16} cm^2$. The finalized design has been optimized for a differential gain of $6.1 \times 10^{-16} cm^2$, having a minimized turn on delay, with a modulation bandwidth of 15.1 GHz and an output power of 71.38 *mW*.

Keywords: Red Laser Diode, SCH, MQW, Modulation Response, Differential Gain.

1 INTRODUCTION

Laser Diodes operating at around 635*nm* wavelength have several applications including optical disk recording read/write application (Lu et al., 1998; Smowton et al., 2003), sensor applications, display technologies (Gauggel et al., 1997) and medical science (photo dynamic therapy) (Smowton et al., 2003; Charamisinau et al., 2005; Mustafa et al., 2011; Rossi et al., 2011).

The first demonstration of the red emission wavelength laser was done during the 1985 using GaInP/AlGaInP material system (Qiu et al., 2008). Quantum Well (QW) diode lasers fabricated in the GaInP/AlGaInP material system covers the wavelength range of 630–690*nm*. Although these devices are available as commercial products, it is clear that their threshold current increases linearly with temperature and that the external differential quantum efficiency above threshold decreases with increasing temperature. These unwanted characteristics become particularly pronounced as the operating wavelength is reduced and they present one of the major barriers to the reproducible fabrication of devices in the region of 630*nm*, especially when reasonable output power is required (Wood et al., 2000).

The carrier confinement in GaInP/AlGaInP quantum wells of the single heterostructure, especially the electron confinement, has been reported to be very poor due to AlGaInP having a maximum allowable direct bandgap of only about 2.32*eV* (Qiu et al., 2008). For improving the carrier confinement near the active region and photon confinement within the cavity, double heterostructure has been implemented. The double-heterostructure laser was first demonstrated during the 1970s (Alferov et al., 1998).The differential gain *dg/dN* is an important parameter in high speed laser application. This is primarily because the relaxation resonance frequency of the laser depends on the square root of the differential gain (Coldren et al., 1995). So ideally, higher differential gain can improve the modulation response of the laser. Furthermore variation of differential gain directly affects the rate equations as well.
In this paper, the performance analysis and optimization of a 635*nm* $Ga_{0.5}In_{0.5}P/(Al_{0.5}Ga_{0.5})_{0.5}In_{0.5}P$ MQW edge emitting laser are presented considering the effects of variation of differential gain.

2 STRUCTURE AND DESIGN OF A 635*nm* MQW RED LASER

For designing a 635*nm* Red laser, GaInP is selected as an active layer material. For achieving high performance, the concentrations of this QW material are selected from the results obtained after computation using Vegard's law (Vurgaftman et al., 2001). The results are found to coincide with other research works. The active region of the laser presented in fig.1 consists 3 QWs of 80*Å* each which are separated by $(Al_{0.5}Ga_{0.5})_{0.5}In_{0.5}P$ barriers of thickness 100*Å* each. At 300K, the bandgap energies of the $Ga_{0.5}In_{0.5}P$ QW material, $(Al_{0.5}Ga_{0.5})_{0.5}In_{0.5}P$ barrier and Separate Confinement Heterostructure (SCH) material are obtained as 1.955*eV* and 2.315*eV* respectively with the well known equations (Chow et al., 1999; Adachi et al., 2005).

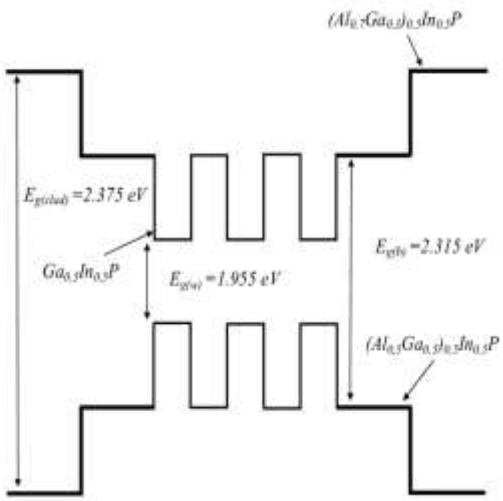

Fig. 1. The active region of a SCH Red Laser consisting 3 quantum wells of 80*Å* each.

Fig. 2. The structure of a designed 635*nm* MQW Red Laser.

The active region is sandwiched by SCH layer of $(Al_{0.5}Ga_{0.5})_{0.5}In_{0.5}P$ material having a thickness of 900*Å* each which are enclosed within cladding layers of $(Al_{0.7}Ga_{0.3})_{0.5}In_{0.5}P$ doped material. The length and width of the cavity are 900μm and 2μm respectively. The ends of the device are cleaved to form flat planes called 'facets' that act as partially reflective mirrors allowing an achievement of reflectivity of 33.5%. Current is injected through the upper p-type contact of the device and leaves through the lower n-type contact, connected at the bottom of GaAs substrate as shown in fig.2.

Calculations of Material Gain

For the active region material, the optical gain has to be obtained in order to design a practical laser. This is done by computing the gain at the operating wavelength and also within a fine range around it. The material gain is expressed as (Coldren et al., 1995; Basak et al., 2011)

$$g(E) = \left(\frac{q^2\pi\hbar}{\varepsilon_0 m_0{}^2 n_r c E}\right)|M_T|^2 \rho_r (f_2 - f_1) \quad (1)$$

where, q is the electronic charge, ε_0 is the free space permittivity, c is the speed of light, n_r is the refractive index of the laser structure, E is the transition energy, m_0 is the stationary mass of electron, $|M_T|^2$ is the square of the transition momentum matrix element, ρ_r is the reduced density of state, $\hbar$ is the Planck's constant divided by 2π, f_2 and f_1 are quasi-Fermi functions in the conduction and valance band respectively.
Using equation (1), at 300K the material gain for a 635nm $Ga_{0.5}In_{0.5}P/(Al_{0.5}Ga_{0.5})_{0.5}In_{0.5}P$ 80$\AA$ MQW SCH Red Laser is calculated, using MATLAB, by varying wavelength. It is essential to arrange so that the cavity oscillation occurs at the peak value of the gain of the material. The obtained results are plotted as shown in fig.3. A peak material gain value of 766.6 cm^{-1} is obtained for the $Ga_{0.5}In_{0.5}P/(Al_{0.5}Ga_{0.5})_{0.5}In_{0.5}P$ MQW SCH EEL around the lasing wavelength of 610nm.

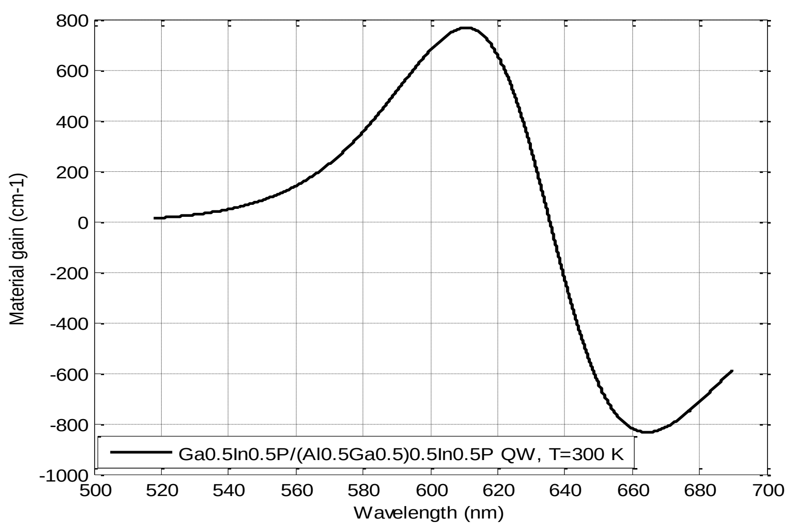

Fig. 3. Plot of material gain vs. wavelength of the designed $Ga_{0.5}In_{0.5}P/(Al_{0.5}Ga_{0.5})_{0.5}In_{0.5}P$ 3QW SCH edge emitting laser at 300K. The material gain of the designed laser varies with the variation of wavelength and a maximum gain is obtained as 766.6 cm^{-1} at 610nm wavelength.

Using the obtained value of the peak material gain the performance characteristics of the designed 635nm SCH edge emitting red laser have been presented in the following section.
A high peak material gain with lower transparency carrier density of a QW material is required for designing a semiconductor laser. The transparency carrier density (N_{tr}) of a material is related to the effective masses of carriers in the conduction band (CB) and valance band (VB) as (Coldren et al., 1995; Basak et al., 2011)

$$N_{tr} = 2\left(\frac{kT}{2\pi\hbar^2}\right)^{3/2}(m_c m_v)^{3/4} \qquad (2)$$

where, k is the Boltzmann constant, T is the temperature in Kelvin, $\hbar$ is the rationalized Planck's constant, m_c and m_v are the effective masses of the carriers in the CB and VB respectively.

At 300K, the calculated value of transparency carrier density of $Ga_{0.5}In_{0.5}P$ QW material is $1.1513 \times 10^{18}\ cm^{-3}$, where, the effective mass of carriers in CB is $0.092m_0$ and the effective mass of carriers in VB is $0.179m_0$, here, m_0 is the mass of electron. This value of N_{tr} is lower than that of the barrier material for which it is suitable to use itself as the QW material.

3 PERFORMANCE CHARECTRISTICS OF THE DESIGNED RED LASER

The performance characteristics of the designed RED Laser are obtained in this work using MATLAB simulation.

3.1 Computations of threshold carrier density (N_{th}), photon life time (τ_p), threshold current (I_{th}) and output power (P_0) of the designed laser

At 300K, the threshold carrier density of $1.2902 \times 10^{18}\ cm^{-3}$ have been found out using the well known expression (Coldren et al., 1995). The photon lifetime (τ_p) is then obtained using the well known expression as $6.637\ ps$ from a group velocity v_g of $8.7848 \times 10^9\ cms^{-1}$.

The threshold current is then calculated using (Coldren et al., 1995)

$$I_{th} = \frac{q \times V \times N_{th}}{\eta_i \times \tau_c} \qquad (3)$$

It is found that at 300K the threshold current is as low as $6.7\ mA$ with an injection current efficiency (η_i) of 0.9, carrier lifetime (τ_c) of $2.71 \times 10^{-9}\ s$ and the active region volume (V) of $7.92 \times 10^{-11}\ cm^3$.

The output power of the designed laser can also be calculated by varying the injection current as (Coldren et al., 1995)

$$P_o = \frac{\alpha_m h v \eta_i}{q g \Gamma}(I - I_{th}) \qquad (4)$$

where, g is the material gain, α_m is the mirror loss coefficient, h is the Planck's constant, v is the lasing frequency, Γ is the confinement factor, I is the injection current and I_{th} is the threshold current.

The obtained results are presented as shown in fig.4. Here, the cavity volume (V_p) of the device is $4.032 \times 10^{-10}\ cm^3$ and the confinement factor (Γ) is 0.1964.

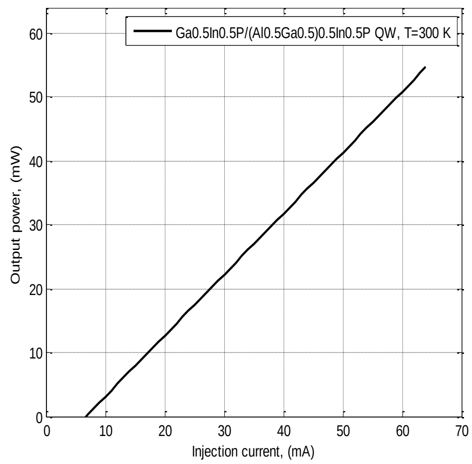

Fig. 4. Plot of output power vs. injection current of the designed $Ga_{0.5}In_{0.5}P/(Al_{0.5}Ga_{0.5})_{0.5}In_{0.5}P$ 80*Å* 635*nm* Red laser.

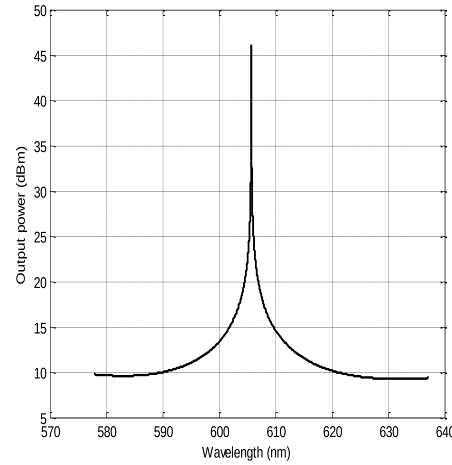

Fig. 5. Plot of output power vs. wavelength of the designed laser at 300K, where the injection current is 64 *mA*. A peak intensity of the power is obtained at 605.7*nm* wavelength.

From fig.4 it is found that after the threshold current of 6.7 *mA*, the output power of the laser increases linearly with the increase of injection current.
For a fixed value of injection current of 64 *mA*, the output power of the laser is also calculated by varying wavelength using equation (4) and the obtained results are plotted as shown in fig.5. Here, the differential gain of the device is taken as $5.1 \times 10^{-16}\ cm^2$. It is found that the material gain of the laser varies with the change in wavelength; as a result, the output power of the laser also varies as equation (4). At 300K for a value of injection current of 64 *mA*, the peak intensity of output power of the designed edge emitting laser is obtained at 605.7*nm* wavelength as shown in fig.5.

3.2 Modulation Response of the designed laser

The modulation response of the designed laser has been obtained using the equation of the transfer function as given below (Coldren et al., 1995; Basak et al., 2011)

$$H(f) = \frac{{f_R}^2}{{f_R}^2 - f^2 + j\frac{f}{2\pi}\gamma} \qquad (5)$$

where, f_R is the resonance frequency and γ is the damping parameter of the laser.

The above equation has been used to obtain the plot of relative response vs. frequency for a value of injection current of 64 *mA* as shown in fig.6.

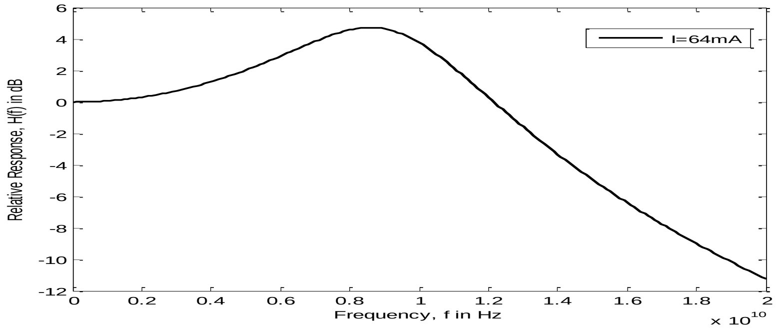

Fig. 6. Plot of relative response vs. frequency of $Ga_{0.5}In_{0.5}P/(Al_{0.5}Ga_{0.5})_{0.5}In_{0.5}P$ 80*Å* MQW Red Laser at 300K with an injection current of 64 *mA*.

It is found that the resonance frequency of the device is 8.6 GHz and the modulation bandwidth is obtained as 13.85 GHz at 64 *mA* injection current.

4 EFFECTS OF DIFFERENTIAL GAIN VARIATION ON THE PERFORMANCE OF THE DESIGNED LASER

In this section, the effects of variation of differential gain on the performance characteristics of the designed laser have been presented. Theoretical study of quantum well structure reveals that a very low value of differential gain causes the laser to reach its threshold level at a higher time while a high differential gain value allows the laser to reach threshold at a lower value of time but at the expense of lower steady state carrier density (Coldren et al., 1995). The solution of the rate of change of carrier density and the rate of change of photon density (Coldren et al., 1995; Schaer et al., 2003; Dezhi et al., 2012) of the designed laser have been obtained using the parameter values (Coldren et al., 1995; Vurgaftman et al., 2001; Chow et al., 1999; Adachi et al., 2005), for a time window of 0-3*ns* approximately using finite difference method in MATLAB for a chosen value of injection current of 64 *mA*.

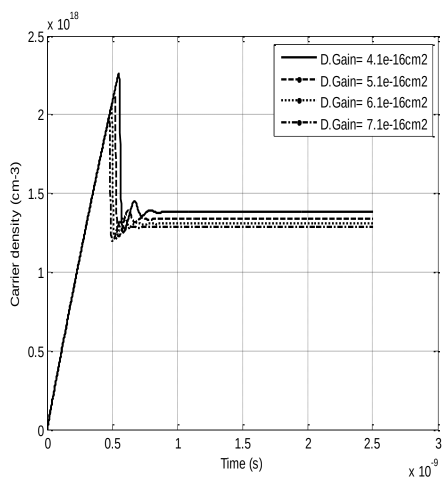

Fig. 7. Plots of carrier density vs. time of the designed 635*nm* laser by varying differential gain.

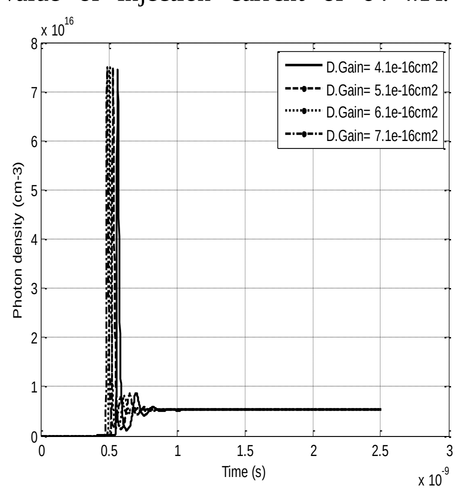

Fig. 8. Plots of photon density vs. time of the designed 635*nm* laser by varying differential gain.

.

In this work, the differential gain of the device is varied from $4.1 \times 10^{-16} cm^2$ to $7.1 \times 10^{-16} cm^2$. Fig.7 shows the effect of varying differential gain on the carrier density vs. time plot of the designed Red laser.

From fig.7 it is observed that with the increase in differential gain the steady state carrier density decreases.

Fig.8 represents the effect of variation of differential gain on the photon density vs. time plot.

From fig.8 it is observed that with the increase of differential gain, the photon density of the laser sligntly increases which minimize the turn on delay of the device.

In fig.9 the effects of varying differential gain on the output power vs. time has been presented.

From fig.9 it is found that the output power of the laser increases slightly with the increase in the differential gain.

The modal gain (i.e. confinement of material gain) of an edge emitting laser can be computed using the following equation (Coldren et al., 1995)

$$\Gamma g = \Gamma g_0 \ln\left(\frac{N}{N_{tr}}\right) \qquad (6)$$

where, g_0 is the peak material gain of the active region material and N is the carrier density of the laser.

Fig.10 presents the change in the modal gain vs. time characteristics due to the effects of differential gain variation.

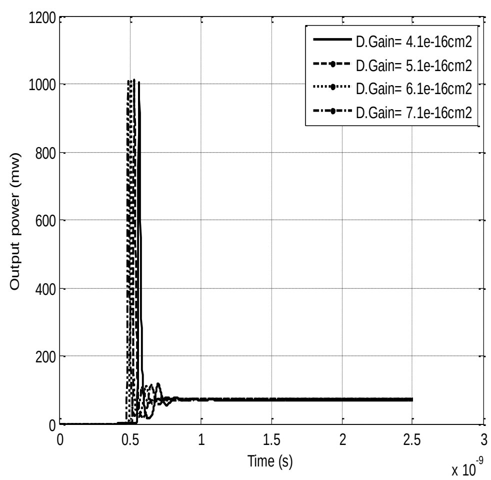

Fig. 9. Plots of output power vs. time of the designed 635*nm* laser by varying differential gain.

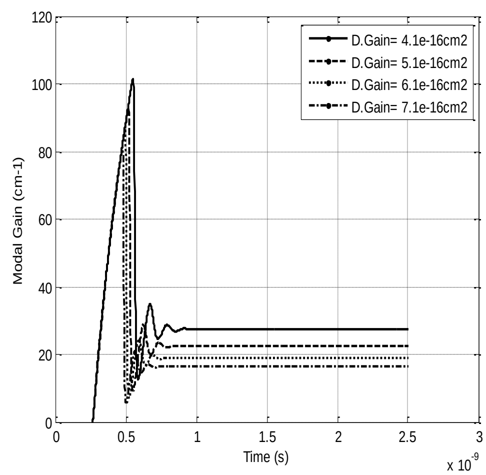

Fig. 10. Plots of modal gain vs. time of the designed 635*nm* laser by varying differential gain.

The modal gain of the device is found to decrease significantly with the increase in differential gain as shown in fig.10.

In fig.11 the effects of varying the differential gain on the relative response of the designed 635*nm* laser has been presented using equation (5).

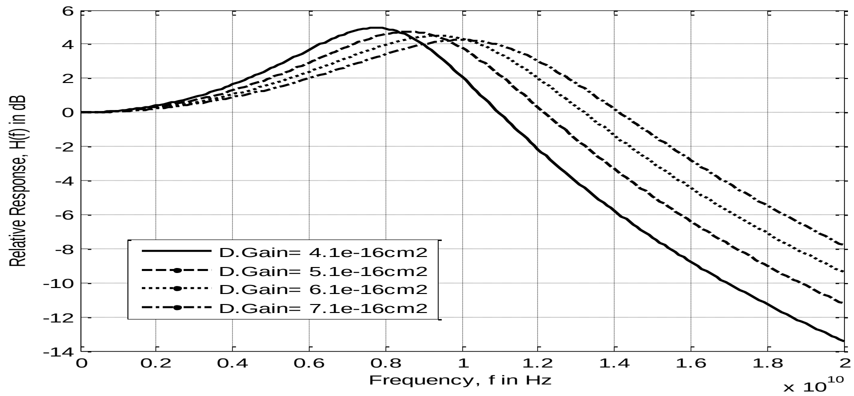

Fig.11. Plots of relative response vs. frequency of $Ga_{0.5}In_{0.5}P/(Al_{0.5}Ga_{0.5})_{0.5}In_{0.5}P$ 80Å 3QW Red Laser at 300K for different values of differential gain.

A maximum relaxation resonance frequency of 10 GHz and modulation bandwidth of 16.15 GHz of the laser are obtained with the differential gain of $7.1 \times 10^{-16} cm^2$ as shown in fig.11.
The results obtained in this performance evaluation with the variation of differential gain has been tabulated in table-1.

TABLE 1- **Results obtained from the performance analysis of the designed laser by varying differential gain.**

Differential Gain (cm^2)	4.1×10^{-16}	5.1×10^{-16}	6.1×10^{-16}	7.1×10^{-16}
Steady State Carrier Density (cm^{-3})	1.381×10^{18}	1.336×10^{18}	1.306×10^{18}	1.284×10^{18}
Steady State Photon Density (cm^{-3})	5.261×10^{15}	5.283×10^{15}	5.293×10^{15}	5.308×10^{15}
Steady State Output Power (mW)	70.89	71.18	71.38	71.52
Steady State Modal Gain (cm^{-1})	27.4	22.41	18.96	16.44
Resonance Frequency (GHz)	7.8	8.6	9.3	10
-3dB Bandwidth (GHz)	12.4	13.85	15.1	16.15

As found in earlier computation, the threshold carrier density of the device is $1.2902 \times 10^{18}\ cm^{-3}$. From table - 1 it is found that with the increase in the differential gain up to $7.1 \times 10^{-16}\ cm^2$, the steady state carrier density of $1.284 \times 10^{18} cm^{-3}$ falls below the threshold value. So at this value of differential gain the lasing mechanism does not sustain. After further computations in this work it is found that the maximum allowable differential gain at 300K temperature with a steady state carrier density above the threshold is at around $6.7 \times 10^{-16} cm^2$. At this value of differential gain, the steady state carrier density is $1.292 \times 10^{18}\ cm^{-3}$, the steady state photon density is $5.304 \times 10^{15} cm^{-3}$, the output power of the laser is 71.47 mW, the relaxation resonance frequency is 9.8 GHz and the corresponding modulation bandwidth is 15.75 GHz.

5 CONCLUSION

In this work, the dimensions of the 635nm 3QW SCH edge emitting Red laser along with the widths of quantum wells and separate confinement heterostructure have been optimized. The material gain of the $Ga_{0.5}In_{0.5}P/(Al_{0.5}Ga_{0.5})_{0.5}In_{0.5}P$ MQW SCH edge emitting laser has been computed to be $766.6\ cm^{-1}$ for obtaining the performance characteristics of the laser.
At 300K, the threshold current of the laser is found out to be 6.7 mA. A maximum steady state output power of 71.18 mW has been computed. A maximum steady state carrier density has been found out to be $1.336 \times 10^{18} cm^{-3}$ which is well above the threshold carrier density of $1.2902 \times 10^{18} cm^{-3}$ and transparency carrier density of $1.152 \times 10^{18} cm^{-3}$. A maximum relaxation resonance frequency of 8.6 GHz and the corresponding modulation bandwidth of 13.85 GHz at an injection current of 64 mA have been found for the three quantum well structure with a differential gain of $5.1 \times 10^{-16}\ \mathrm{cm}^2$.
Furthermore the performance analysis reveals that the key performance characteristics such as the output power, resonance frequency and modulation bandwidth increases with the increase in differential gain. It has been also found that the turn on delay, the steady state carrier density and the modal gain also decreases with the increase in the differential gain. The maximum allowable differential gain at 300K is $6.7 \times 10^{-16} cm^2$. Above this value of differential gain, the steady state carrier density falls below the threshold carrier density, causing the lasing action to stop. As a result, the designed laser is optimized for a differential gain of $6.1 \times 10^{-16}\ \mathrm{cm}^2$, for its better performance having an acceptable minimized turn on delay with a maximum relaxation resonance frequency of 9.3 GHz and a modulation bandwidth of 15.1 GHz, having a output power of 71.38 mW. The designed 635nm MQW laser is expected to perform well after fabrication. However, the design is the first of its kind designed without considering thermal degradation and some other performance parameters such as noise intensities (RIN and FM noise) due to which scopes of development and improvement are still open for achieving a better performance.

REFERENCES

Lu, B., Vail, E., Osinski, J.S. & Schmitt, B. (1998). High-speed low-parasitic low-divergence 635nm single mode lasers. *Electronics Letters, 34*(*18*), 1750-1751.

Smowton , P. M., Lewis, G. M., Blood, P. & Chow, W. W. (2003). Optimization of 635-nm Tensile Strained GaInP Laser Diodes. *IEEE Journal of Selected Topics In Quantum Electronics, 9*(*5*), 1246-1251.

Gauggel, H.P., Winterhoff, R., Kuhn, J., Scholz, F. & Schweizer, H. (1997). Room temperature operation of single mode DBR lasers at 635nm, *Electronics Letters, 33*(*17*), 1466-1467.

Charamisinau, I., Happawana, G. S., Evans, G. A., Kirk, J. B., Bour, D. P., Rosen ,A. & His, R. A. (2005). High-Power Semiconductor Red Laser Arrays for Use in Photodynamic Therapy . *IEEE Journal Of Selected Topics In Quantum Electronics, 11*(*4*), 881-891.

Mustafa, F.H., Jaafar, M.S., Ismail, A.H. & Houssein, H.A.A. (2011). The effect of laser wavelength in photodynamic therapy and phototherapy for superficial skin diseases. *IEEE International Conference on Imaging Systems and Techniques (IST), DOI:10.1109/IST.2011.5962166*, 232-236.

Rossi, R., Lotti, T. & Bruscino, N. (2011). Photodynamic Therapy/Assisted Photo rejuvenation. *Journal of Cosmetics, Dermatological Sciences and Applications*, *1*, 30-35.

Qiu, B., McDougall, S. & Yanson, D. (2008). Analysis of thermal performance of InGaP/InGaAlP quantum wells for high-power red laser diodes. *International Conference on Numerical Simulation of Optoelectronic Devices (NUSOD'08), DOI:10.1109/NUSOD.2008.4668246*, 69-70.

Wood, S. A., Molloy, C. H., Smowton, P. M., Blood, P. & Button, C. C. (2000). Minority Carrier Effects in GaInP Laser Diodes. *IEEE Journal of Quantum Electronics, 36*(*6*), 742-750.

Alferov, Zh. I. (1998). The history and future of semiconductor heterostructures. *American Institute of Physics, Semiconductors, 32*(*1*), 1-18.

Coldren, L. A. & Corzine, S.W. (1995). *Diode Lasers and Photonic Integrated Circuits*, John Wiley & Sons, Inc, 1-263.

Vurgaftman, I., Meyer, J. R. & Ram-Mohan, L. R. (2001). Band parameters for III–V compound semiconductors and their alloys. *Journal of Applied Physics, 89*(*11*), *DOI:10.1063/1.1368156*, 5851-5862.

Chow, W. W. & Koch, S. W. (1999). *Semiconductor-Laser Fundamentals Physics of the Gain Materials*, ISBN 3-540-64166-1 Springer-Verlag Berlin Heidelberg, New York, 210-225.

Adachi, S. (2005). *Properties of group-IV, III–V and II–VI Semiconductors*, John Wiley & Sons, ISBN 0-470-09032-4, 11-359.

Basak, R. & Islam, S. (2011). Performance Analysis of 980 nm $In_{0.2}Ga_{0.8}As$/GaAs MQW VCSEL Considering Thermal Effect. *The AIUB Journal of Science and Engineering (AJSE)*, *10*(*1*), 9-14.

Schaer, T., Rusnov, R., Eagle, S., Jastrebski, J., Albanese, S. & Fernando, X. (2003). A Dynamic Simulation Model for Semiconductor Laser Diodes. *IEEE Canadian Conference on Electrical and Computer Engineering (CCECE)*, 293-297.

Dezhi, X., Wenzhe, W., Xiaoli, J., Jing, S. & Hongxia, L. (2012). A Numerical Model for Semiconductor Laser Diodes. *Symposium on Photonics and Optoelectronics (SOPO), DOI:10.1109/SOPO.2012.6271033*,1-4.

Tawsif Ibne Alam received B.Sc. Engg. (EEE) degree from American International University-Bangladesh (AIUB) Dhaka, Bangladesh in January 2013. Currently is enrolled in M.Sc. Engg. (EEE) degree program in the same university. His research interest includes short wavelength lasers, Red Laser, Blue Laser and embedded systems.

Rinku Basak received B.Sc. Engg. (EEE) degree from Khulna University of Engineering & Technology (KUET) Khulna, Bangladesh in 2004. He received M.Sc. Engg. (EEE) degree from Bangladesh University of Engineering & Technology (BUET) Dhaka, Bangladesh in October 2007. Currently he is working as Head (Graduate Program) of the Dept. of EEE of AIUB. Mr. Basak is a Member of IEEE USA and the Institution of Engineers Bangladesh (IEB). His research interests are on high power and high speed VCSELs, Violet Laser, Blue Violet Laser, True Blue Laser and Red Laser.